Article

Comparative study on the thermal properties of engine oils and their nanofluids incorporating Fullerene-C60, TiO2, and Fe2O3 at different temperatures

Kaveenga Rasika Koswattage [*] , Chanaka Galpaya , Ashan Induranga , Vimukthi Vithanage , M. M. M. G. P. G. Mantilaka

Article

Comparative Study on the Thermal Properties of Engine Oils and Their Nanofluids Incorporating Fullerene-C60, TiO2, and Fe2O3 at Different Temperatures

Chanaka Galpaya [1,2,3], **Ashan Induranga** [1,2,3], **Vimukthi Vithanage** [1,2,3], **Prasanga Mantilaka** [3] and **Kaveenga Rasika Koswattage** [2,3,*]

[1] Faculty of Graduate Studies, Sabaragamuwa University of Sri Lanka, Belihuloya 70140, Sri Lanka; chanakagalpaya@gmail.com (C.G.); ashaninduranga@tech.sab.ac.lk (A.I.); vimukthi@tech.sa.ac.lk (V.V.); mantilaka@gmail.com (P.M.)

[2] Faculty of Technology, Sabaragamuwa University of Sri Lanka, Belihuloya 70140, Sri Lanka

[3] Center for Nano Device Fabrication and Characterization (CNFC), Faculty of Technology, Sabaragamuwa University of Sri Lanka, Belihuloya 70140, Sri Lanka

[*] Correspondence: koswattagekr@appsc.sab.ac.lk

Abstract: The efficiency, durability, and overall performance of a car engine are influenced by several critical factors. The quality and properties of engine oil play a crucial role, and oil is used in internal combustion engines for lubrication and cooling purposes. This research study aimed to compare the impact of fullerene-C_{60} (99.5%), Fe_2O_3, and TiO_2 nanoparticles on the thermal properties of C.A.L.T.E.X. red engine oil with grades 10W30, 20W40, and 20W50. This study focused on the effect of a nanoparticle concentration of 0.01 wt.% in different engine oil grades at various temperature values of 30-120 ℃. The Nanofluids were prepared using the two-step direct mixing method, employing a magnetic stirrer and an ultrasonicator, ensuring uniform distribution of nanoparticles in the base fluids. The thermal conductivity, thermal diffusivity, and volumetric heat capacity of the base fluids and nanofluids were measured using the FLUCON LAMBDA thermal conductivity meter. Additionally, flash points were measured using the flash point tester. It was concluded that the thermal properties of TiO_2 and Fe_2O_3 showed considerable enhancement; in contrast, Fullerene only showed the 212 ℃ flash point.

Keywords: CALTEX red engine oil; nanofluids; thermal conductivity; thermal diffusivity; volumetric heat capacity; flashpoint

1. Introduction

The primary role of the engine oil is to lubricate the engine parts. These parts are constantly subject to friction while the engine is running, and oils wear on the engine parts. Additionally, engine oil is used in all internal combustion engines and industrial machines to prevent corrosion of the components [1]. Furthermore, engine oils serve multiple functions, such as reducing corrosion and friction, cooling and dissipating heat from the engine, as well as sealing the engine parts [2–4]. The overall idea of the engine oil is used to improve the engine efficiency and durability while reducing fuel consumption. However, cooling and dissipation of the heat from the engine are significant roles performed by engine oils, and their thermal properties are such important factors in achieving appropriate performances. Therefore, the thermal properties of engine oil play a critical role in determining its suitability for specific applications. Generally, engine oils contain a complex collection of additives to improve fluid performance. Thermal properties such as thermal conductivity, thermal diffusivity, volumetric heat capacity, and flash point engine oil play a crucial role in enhancing engine performance; for example, oils with higher thermal conductivity facilitate more efficient heat transfer. However, such thermal properties of base engine oils are insufficient to

fulfill the engine performance. Therefore, numerous studies have been conducted to uplift the thermal properties of engine oil by researchers, and one well-known method involves incorporating solid materials with high thermal properties into the base fluid [5–7]. In heat transfer applications, solid particles show higher thermal conductivity compared with conventional fluids [1]. Several parameters of solid materials influence the increase of engine oil's thermal properties, such as particle size, shape, temperature, surfactants, type and duration of ultrasonication, and accumulation of particles [8–10].

There are two primary nanoparticle families have been investigated for nanofluids; metal-based nanoparticles (metals, metal oxides, ex: CuO, TiO_2, SiO_2, ZnO, ZrO_2, Fe_2O_3) and carbon-based nanoparticles (nanographene, nanodiamonds, carbon nanotubes, and graphene species) [11]. Recently, nanoparticles have attracted much research attention as the most promising additives, as even a low concentration of nanoparticles in engine oil is sufficient to enhance its thermal properties. However, studies have indicated that although adding nanofluids improves engine oils thermal properties, the degree of the enhancement depends on factors such as nanoparticle size and shape, concentration, temperature, ultrasonication time and stirring time, surfactants, and base oil [1].

To the best of our knowledge, only one previous study has been conducted to investigate the direct addition of Fullerene (C_{60}) into engine oil to prepare nanofluids and measure the thermal properties [12]; however, there was another study about Fullerene (C_{60}) – SiO_2 hybrid nanoparticles added to engine oil to enhance its thermal properties. In that study conducted by Rostamian et al. [13], it was reported that the addition of Fullerene –SiO_2 hybrid nanoparticle (volume fraction 1%) to 5W30 engine oil increased its thermal conductivity by 9%. Titanium dioxide (TiO_2) is a highly important metal oxide in experimental investigations due to its properties, such as electronic structures and wide band gap. TiO_2 has mainly three crystal structures: anatase (tetragonal, space group I41/amd), rutile (tetragonal, space group P42/mnm), and brookite (orthorhombic, space group Pbca). The anatase-type TiO_2 nanoparticles were used for this research work. Sukkar et al. investigated TiO_2-added nanofluids' thermal conductivity, and the flash point was shown such enhancement but not more than CuO-added nanofluids. However, TiO_2 with 0.1 wt.% nanofluid thermal conductivity and flash point concentration was increased by 4.54% and 9.3%, respectively [14]. Furthermore, Birleanu et al. conducted a study to investigate tribological properties such as load-carrying capacity and friction reduction of nanofluids. They found that the anti-wear abilities of the nanofluids improved by adding surface-modified TiO_2 nanoparticles at 75 °C, and the rate of improvement was increased with the volume concentration (0.01%, 0.02%, 0.05%, and 0.075%) of nanoparticles added [15]. Harandi et al. [16], reported that the 30% increase in the conductivity coefficient at a temperature of 50 °C and a volumetric fraction of 2.3% of hybrid nanofluids composed of Fe_2O_3 nanoparticles, multi-walled carbon nanotubes, and ethylene glycol as the base fluids.

There are several mechanisms developed to explain the behavior and thermophysical properties of nanofluids. Some of them are the Brownian motion, nanoparticle clustering, and thermal liquid layering.

Brownian motion is the random movement of the nanoparticles within the base fluid. Brownian creates collides with the nanoparticles and the liquid molecules, which enhances the thermal conductivity of nanofluids. Brownian motion has one of the major impacts on thermal conductivity compared to other mechanisms. This Brownian motion also helps the Thermophoresis effect: particle movement from hot to cold regions. Clustering or aggregation is also a key mechanism that explains the properties of the nanofluids. However, on some occasions, there might be a positive impact from the particle aggregation that creates a thermal bridge to transfer the heat through the fluid. But, on some occasions, this might have a negative effect on the thermal properties of the nanofluid. However, for some nanofluids, this phenomenon makes the nanofluids unstable. The thermal-liquid layer is the thermal bridge between the nanoparticles and the liquid molecules. This layer is formatted by liquid molecules around the nanoparticles. This layer helps to transfer the heat between the two phases of the nanofluid. However, it is required to conduct further study of the mechanisms of nanofluids to explain their complex behavior.

In this study, the thermal conductivity, thermal diffusivity, volumetric heat capacity, and flash point of 10W30, 20W40, and 20W50-based nanofluids with Fullerene (C_{60}), TiO_2, and Fe_2O_3 nanoparticles were examined, and compared the obtained results graphically. The engine oils chosen for this study were 10W30, 20W40, and 20W50 types, which are widely used in lightweight vehicles. The intention of this work is to enhance the thermal properties of these engine oils by adding different types of nanomaterials. The temperature range and the mass concentration were 30-120 °C and 0.01 wt. % respectively. Equal concentrations of the different nanoparticles were utilized, and the nanofluids were prepared using a two-step method.

2. Materials and Methods

2.1. Materials

In this research work, three engine oil grades, namely 10W30, 20W40, and 20W50, were used as the base fluids for the nanofluids. All three grades of engine oils are multi-graded engine oils, and they are graded according to their viscosity values at hot and cold temperatures. The nanofluids prepared using fullerene-C_{60} (99.5%, SIGMA-ALDRICH, St. Louis, Missouri, United States), TiO_2, and Fe_2O_3; with a weight percentage of 0.01 wt.%. The thermophysical properties of the fullerene-C_{60}, TiO_2, and Fe_2O_3 nanoparticles are given in Table 1, whereas the properties of the three selected engine oil grades are given in Table 2.

Table 1. Thermo-physical properties of Fullerene-C_{60}, TiO_2, and Fe_2O_3.

Property	Fullerene	TiO_2	Fe_2O_3
Density	1.65 g/cm³	3.78 g/cm³	5.24 g/cm³
Size	100-200 nm	20-40 nm	30-80 nm
Thermal conductivity (W/mK)	0.2	4	0.58
Purity (%)	99.5	99	98
Appearance	Black powder	White powder	Red-brown powder

In this study, locally available CALTEX red engine oil was chosen as the base fluid because it is a popular product in the field. The weights of the nanoparticles (0.01 wt.%) were calculated using Eq. (1) while measuring the weight of fluids and nanoparticles using the BSA224S-CW (d=0.1 mg) electronic balance. The weights of nanomaterials are presented in Table 3 for different grades of engine oils with a mass fraction of 0.01 wt.%. From each engine oil grade, a volume of 60 ml nanofluid was prepared for each experiment due to the 50±2 ml liquid required to measure flash point using the flash point meter. The 40±2 ml of liquid was used to measure other thermal properties using the thermal conductivity meter.

$$wt\% = x_{c_{60}}/(x_{c_{60}} + y_{basefluid}) \qquad (1)$$

Table 2. Thermo-physical properties of engine oil grades 10W30, 20W40 and 20W50.

Property	10W30	20W40	20W50
Density (Kg/m³) (at 30 °C)	830.74	839.63	842.82
Thermal conductivity (30 °C) (mW/mK)	131.52	134.32	133.98
Thermal conductivity (100 °C) (mW/mk)	124.82	128.04	127.96
Flashpoint (°C)	207.7	211	213.5

After the measurement of the weights of the base fluids, nanofluids, and nanoparticles, the surface temperature values were measured using a thermometer with an accuracy of ±1 °C. The measured nanoparticles were subsequently added to the measured engine oil and placed on a magnetic stirrer for 2 hours at a temperature of 40 °C and 200 rpm to disperse the nanoparticles within the engine oil. After preparing the oil and nanoparticle mixture, the sample was exposed to ultrasonic waves for another 2 hours at 40 °C using an ultrasonicator (Rocker, SONER 210H, AC, 220 V, 50 Hz,

Rocker Scientific Co., Ltd., Kaohsiung City, Taiwan) to disperse all nanoparticles in the engine oil and eliminate their agglomerates. The photographs of the prepared nanofluid, base fluid, and nanoparticles are shown in Figure 1. This preparation method made nanofluids stable for at least two weeks without the risk of sedimentation; therefore, no surfactant was needed for stabilization.
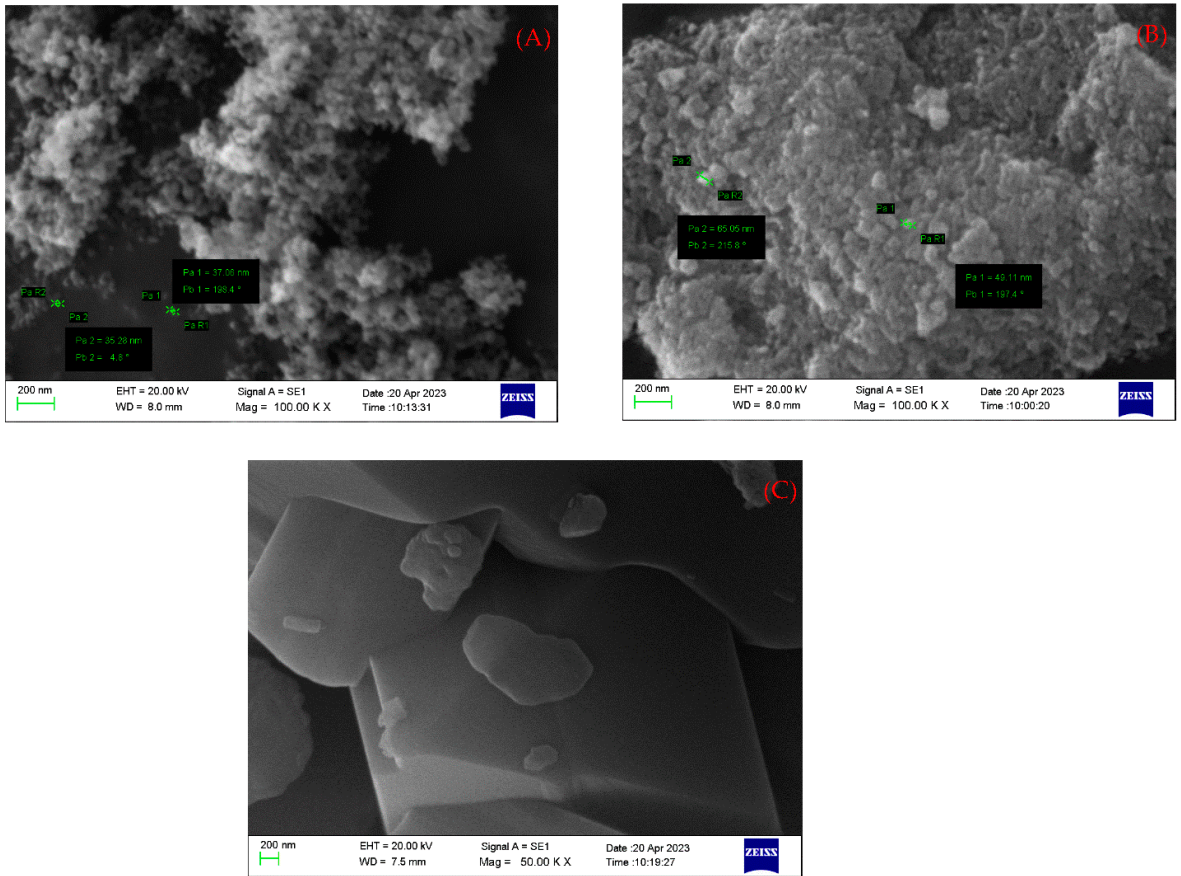

Figure 1. Nanoparticles (a-Fullerene-C_{60}, b-TiO_2, c-Fe_2O_3), base fluid (d-10W30 CALTEX red engine oil), and prepared nano-fluids (e-fullerene-C_{60} 0.01 wt.% added 10W30, f-Fe_2O_3 0.01 wt.% added 10W30, g-TiO_2 0.01 wt.% added 10W30).

Table 3. Weights of nanoparticles for different engine oil grades with 0.01 wt.%.

Engine Oil	Fullerene (g)	TiO_2 (g)	Fe_2O_3 (g)
10W30	0.0040	0.0071	0.0076
20W40	0.0048	-	-
20W50	0.0048	-	-

The Scanning Electron Microscope (SEM) tests were conducted to ensure the surface topography and composition of the nanoparticles. The obtained results are presented in Figure 2.

Figure 2. SEM images of the nanoparticles used in this research work. A: TiO_2. B: Fe_2O_3. C: Fullerene – $C_{60.}$

2.2. Thermal conductivity, Thermal diffusivity, and Volumetric heat capacity measurements

The thermal properties of liquids can be measured using various methods such as the steady state method, temperature oscillation method, transient hot wire method, etc [1]. In this research work, the transient hot-wire method was used to measure thermal properties using the instrument TECNE UCAL 400^+ dry block calibrator and FLUCON Lambda thermal conductivity meter, which can be employed to obtain thermal conductivity and thermal diffusivity of both the base fluids and nanofluids were measured within a temperature range of 30 to 120 ℃.

The LAMBDA Thermal Conductivity Meter uses the hot wire transient method for thermal conductivity, thermal diffusivity, and volumetric heat capacity according to ASTM D7896-19 standardization [17]. LAMBDA thermal conductivity has platinum wire to transfer the heat to liquid.

According to the theory of the hot-wire transient method, it produces a constant heat stream. This heat stream is time-dependent. The Eq. (2), can be developed to calculate the thermal conductivity of the liquid.

$$\lambda = \frac{q}{4\pi(\vartheta_1 - \vartheta_{2)}} ln\left(\frac{t_2}{t_1}\right) \tag{2}$$

where λ is thermal conductivity (Wm^{-1} K^{-1}), q is a constant heat stream (Wm^{-1}), and ϑ is the temperature at time t.

The accuracy of the instrument at a temperature below 200 ℃ is ±0.03 ℃. The volumetric heat capacity of the fluids in each temperature value was calculated using Eq. (3).

$$C_v = \lambda/\alpha \tag{3}$$

$$where, C_v - Volumemetric\ heat\ capacity, \lambda - Thermal\ conductivity, \alpha - Thermal\ diffusivity$$

2.3. Flash point measurement

The flash point of the base fluids and nanofluids was measured using the open-cup flash point tester (Anton Paar PMA500, Germany). The flash point is the lowest temperature at which a liquid forms a gas above its surface in sufficient concentration to ignite. The sample was placed in the test cup and slowly heated up automatically to reach the flash point, and the measuring standard was ASTM D93 [18]. The samples were discarded after measuring the flash point due to the samples' temperature exceeding 200 ℃ degrees.

3. Results and Discussion

Table 4 represents several research works carried out by previous researchers, and it includes the thermal conductivity and flash point percentages of different nanoparticles added to different base fluids with temperature ranges and weight or volume fractions. By looking at Table 4, the engine oil-based nanofluids' thermal conductivity percentage shows considerable enhancement, while GO nanoparticle-added nanofluid took the highest percentage (58%) with low weight fractions at a temperature range of 10-60 ℃. The engine oil-based nanofluids flash point percentage shows significant enhancement, while graphene nanoparticle-added to engine oil-based nanofluids demonstrate the highest percentage (25.4%) with low weight fractions. However, it can be concluded that nanomaterials can make a considerable impact on the thermal properties of different fluids.

Table 4. Summary of the thermal conductivity and flash point of nanofluids examined by previous researchers.

Nanoparticle	Base fluid	Temperature (°C)	Concentration	Thermal conductivity enhancement (%)	Flashpoint enhancement (%)	Ref.
TiO_2	Oil / Virgin mineral oil	25-50	0.1-1	7.08	14.7	[19,20]
Mg/MWCNT	Engine oil	25-60	0.25-2	50	-	[4]
Cu	Oil	40-100	0.2-1 wt.%	49	-	[21]
Mg/MWCNT	10W40	25-50	0.25-2 wt.%	65	-	[22]
WO_3-Ag	Transformer oil	40-100	1-4 wt.%	41	-	[23]
MWCNT	20W50, 20W40	20	0.1-0.5 wt.%, 0.5 wt.%	22.7	10.5	[24,25]
Ag	Engine oil	40-100	0.36-0.72 wt.%	37.1	-	[26]
CuO	20W50	25	0.1-6 wt.%	8.3	7.9	[27,28]
hBN/Al_2O_3	15W40		0.5		-	
Al_2O_3/Fe_2O_3	10W40	25-65	0.25-4	33	-	[1]
rGO	Ethylene glycol	10-60	1.9-9.3	90	-	
GO	Ethylene glycol/SAE50 engine oil	10-60	1.9-9.3/0.01-1 wt.%	58	8	[29,30]
Graphene	Kerosene/5W30 engine oil	20-70	0.0005-0.2 wt.%	23	25.4	[31,32]
SiO_2	Liquid paraffin/20W40 engine oil	25-70	0.005-5 wt.%/0.3-1.5 wt.%	38	6.97	[33,34]
ZnO	SAE50 engine oil	25-55	0.1-1.5 wt.%	8.74	13	[35,36]
TiO_2	10W30 engine oil	30-120	0.01 wt.%	4.5	4.2	This study
Fe_2O_3	10W30 engine oil	30-120	0.01 wt.%	3.9	3.5	This study
Fullerene-C_{60}	10W30 engine oil	30-120	0.01 wt.%	-	2.1	This study

The morphology of the TiO_2 and Fe_2O_3 nanoparticles were spherical to some extent, which provided a good rolling mediator inside engine oil. The SEM images prove that the average particle size of TiO_2, Fe_2O_3, and fullerene-C_{60} is about 30-60 nm, 40-70 nm, and 100-200 nm, respectively.

3.1. Measurements of base fluids

The base fluids' thermal properties were measured using the same instruments at the same temperature range to evaluate the performances of the nano lubricants. The measured thermal conductivity and flash point values of engine oil grades 10W30, 20W40, and 20W50 were compared with their nanofluids.

*3.2. Effect of temperature values and nanomaterials on thermal properties*

3.2.1. Thermal conductivity

Thermal conductivity can be explained as the quality of a material to conduct heat. A large value of thermal conductivity of liquid is considered as a good cooling agent for motor engines. A fluid with high thermal conductivity absorbs further heat in the engine, reduces heat loss, and enhances the performance of the engine. Generally, the thermal conductivity of engine oil is inversely proportional to the temperature due to molecules of the liquid moving apart when a liquid is heated. Hence, their mean free path increases. This leads to a reduced probability of collision of molecules, and therefore, there is a reduction in thermal conductivity with an increase in temperature for liquids. However, when in nanofluids, the nanoparticles will be placed through liquid molecules, reducing

the distance between the two molecules. Therefore, this enhances the interaction, resulting in an increment of the heat exchange within nanofluids. Figure 3 compares the thermal conductivity results of 10W30, 20W40, and 20W50 engine oils with Fullerene (C_{60}) 0.01 wt.% added nanofluids within the 30-120 °C temperature range. Nevertheless, the result of the enhancement of the nanofluid's thermal conductivity does not agree with some other experimental results [20]. However, both base fluid and nanofluid display a decrement in thermal conductivity when the temperature is increased while keeping the graphs' slopes approximately equal. Figures 4 and 5 show the thermal conductivity results of TiO_2 and Fe_2O_3 0.01 wt.% added nanofluids with the base fluid (10W30) results in the temperature range 30-120 °C. Both figures display a substantial improvement in the thermal conductivity values of nanofluids compared to their respective base fluids, i.e., 4.5% and 3.9%, for TiO_2 and Fe_2O_3 added nanofluids, respectively.
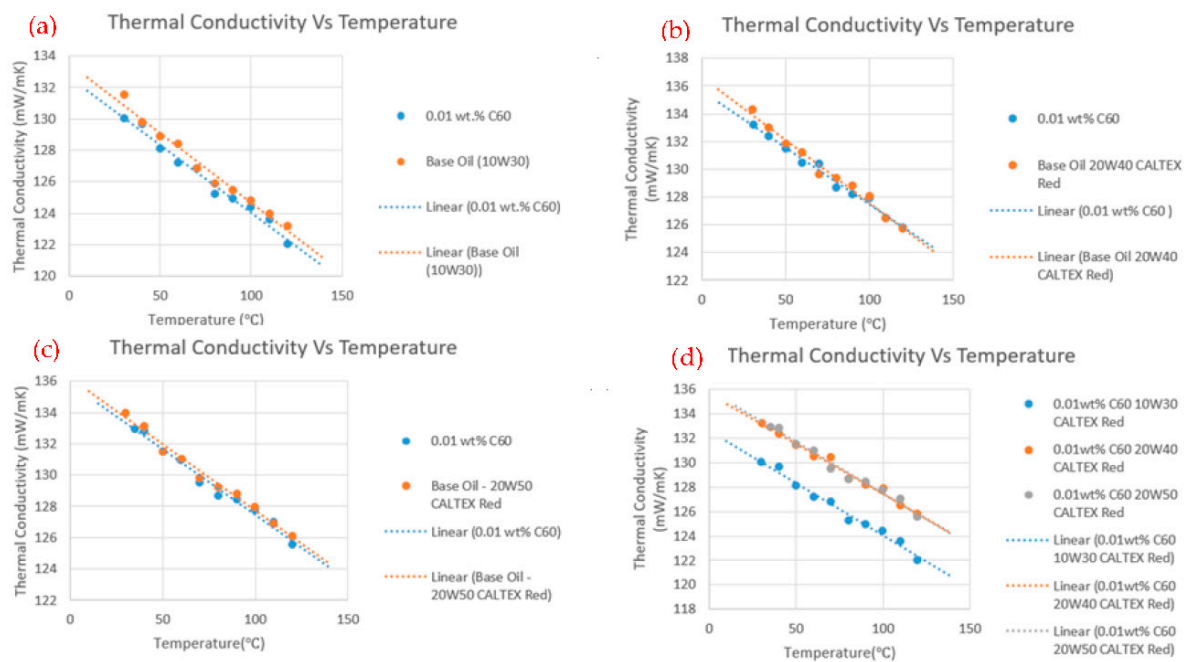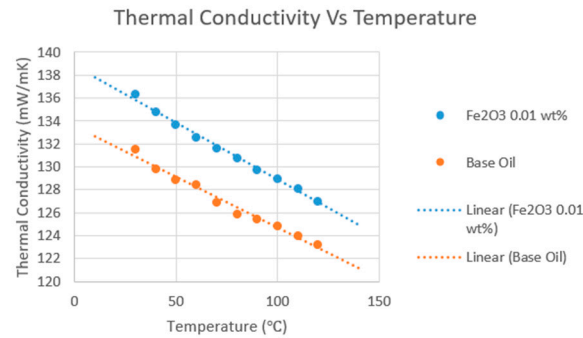

Figure 3. Effect of temperature on thermal conductivity of fullerene-C_{60} 0.01 wt.% added nano-fluids with base fluids (a-10W30, b-20W40, c-20W50, d-comparison of thermal conductivity of three nanofluids).
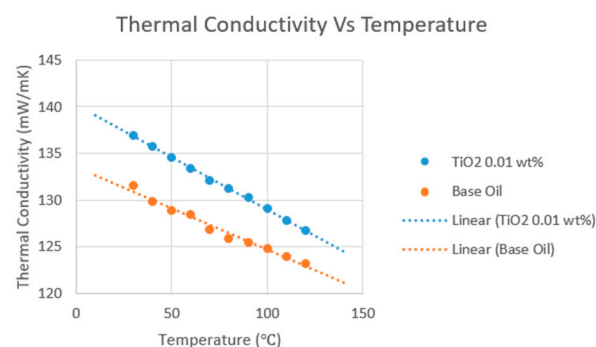
Figure 4. Effect of thermal conductivity on 10W30/TiO_2 0.01 wt.% added nano-fluid.

Figure 5. Effect of thermal conductivity on 10W30/Fe$_2$O$_3$ 0.01 wt.% added nano-fluid.

It can be concluded that the results obtained from this research work consistent with previous studies results.
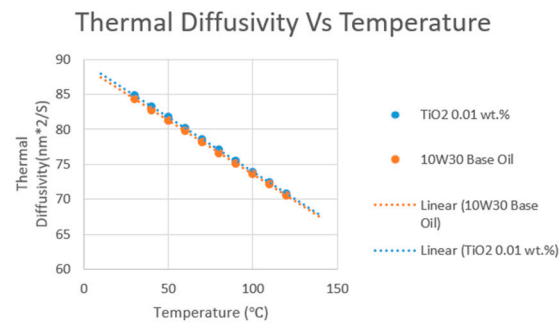
3.2.2. Thermal diffusivity

The rate of heat transfer through a medium is called thermal diffusivity. Figure 6 shows the results of thermal diffusivity values of base fluids 10W30, 20W40, and 20W50 and its Fullerene (C$_{60}$) added nanofluids with mass fraction 0.01 wt.% in the temperature range of 30-120 °C. As is clearly observed in the figure, there was no significant improvement in the thermal diffusivity of C$_{60}$-added nanofluids with the increment of the temperature of the samples compared to their respective base fluids.

The gradients of the graphs for both the base fluid and its nanofluid were nearly equal while decreasing the thermal diffusivity values when increasing the temperature from 30-120 °C. These findings align with theoretical expectations and are consistent with previous studies.

Thermal diffusivity values of TiO$_2$ and Fe$_2$O$_3$ added nanofluids with 0.01 wt.% and base fluid (10W30) values comparison is represented in Figure 7 and Figure 8, respectively. Both graphs exhibit a linear shape and do not show significant enhancements of the thermal diffusivity within the temperature range of 30-120 °C.
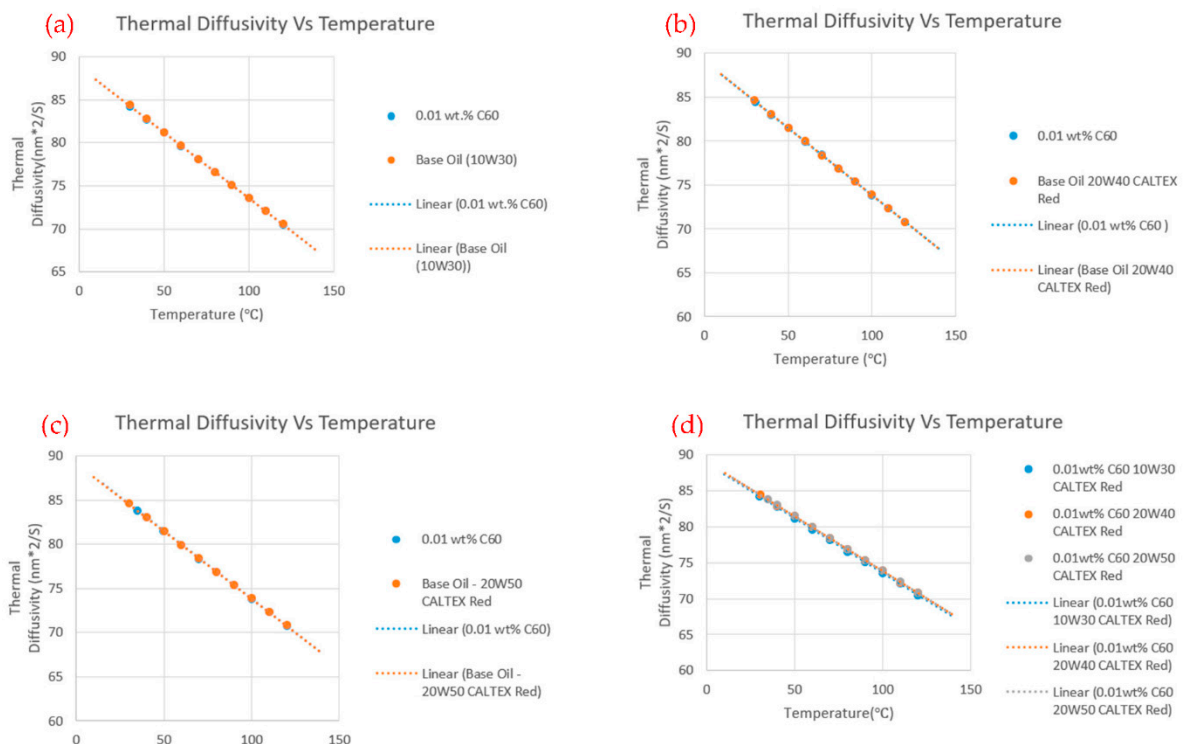
Figure 6. Effect of temperature on thermal diffusivity of fullerene-C_{60} 0.01 wt.% added nano-fluids with base fluids (a-10W30, b-20W40, c-20W50, d-comparison of thermal diffusivity of three nanofluids).
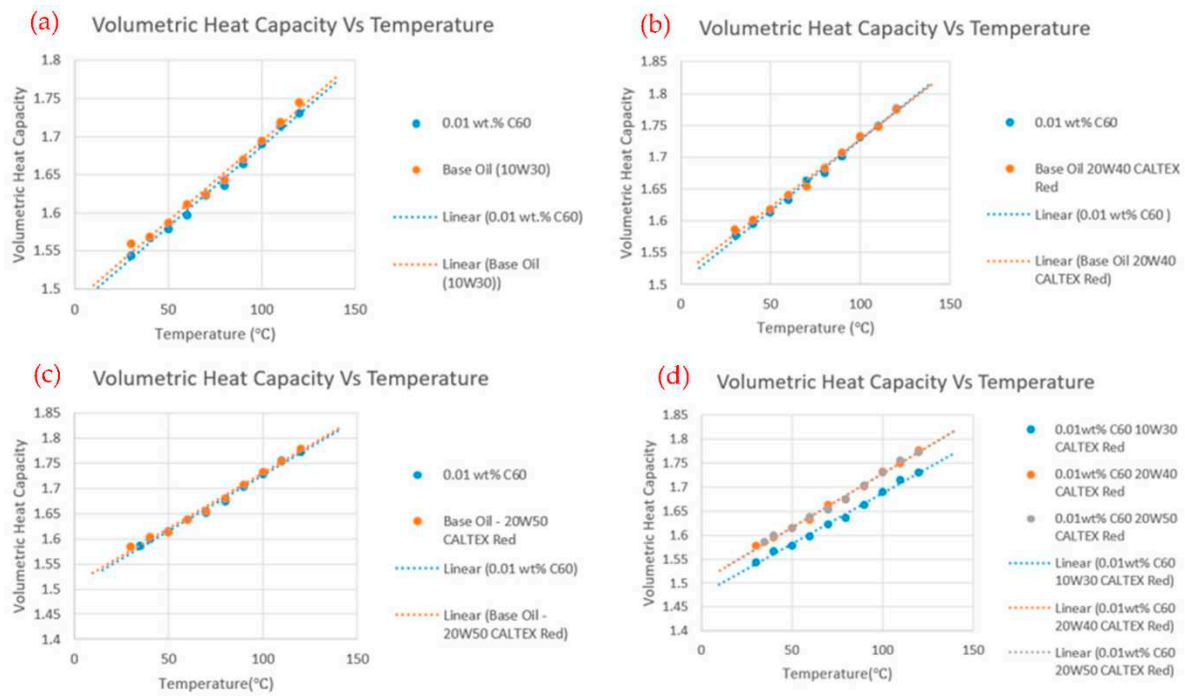

Figure 7. Effect of thermal diffusivity on 10W30/TiO_2 0.01 wt.% added nano-fluid.
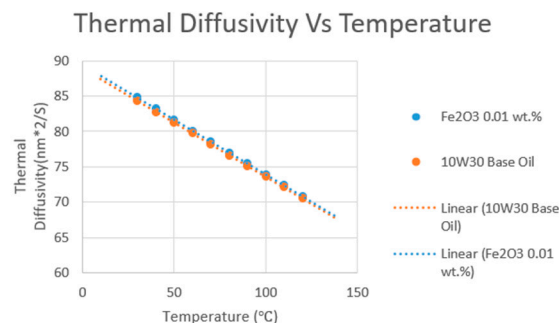
**Figure 8.** Effect of thermal diffusivity on 10W30/Fe_2O_3 0.01 wt.% added nano-fluid.

3.2.3. Volumetric heat capacity

The ratio of thermal conductivity to thermal diffusivity is called volumetric heat capacity. Figure 9 compares the volumetric heat capacity values of base fluids (10W30, 20W40, and 20W50) and Fullerene (C_{60}) based nanofluids with 0.01 wt.% in the temperature range of 30-120 °C. The graph shows an increase in the volumetric heat capacity values of the nanofluids as the temperature of the sample increases. This increase has a positive gradient on the graph, but the enhancement of the values compared to the base fluid is not substantial.

10

Figure 9. Effect of temperature on volumetric heat capacity of fullerene-C_{60} 0.01 wt.% added nano-fluids with base fluids (a-10W30, b-20W40, c-20W50, d-comparison of volumetric heat capacity of three nanofluids).

These results should be expected because the slope of thermal diffusivity graphs is greater than the respective thermal conductivity graph slope. Volumetric heat capacity values of TiO_2 and Fe_2O_3 added nanofluids with 0.01 wt.% and base fluid (10W30) values comparison is represented in Figure 10 and Figure 11, respectively.
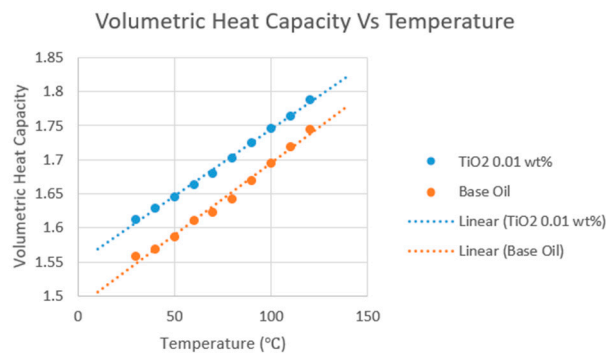
Figure 10. Effect of volumetric heat capacity on 10W30/TiO_2 0.01 wt.% added nano-fluid.
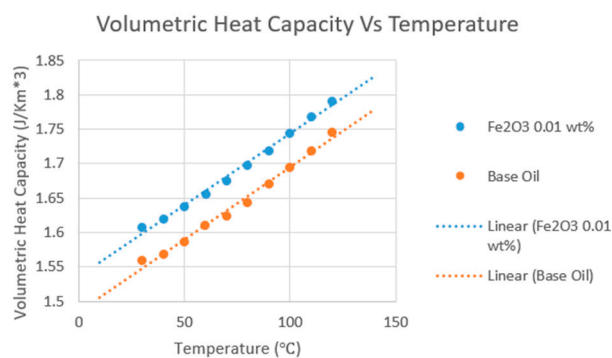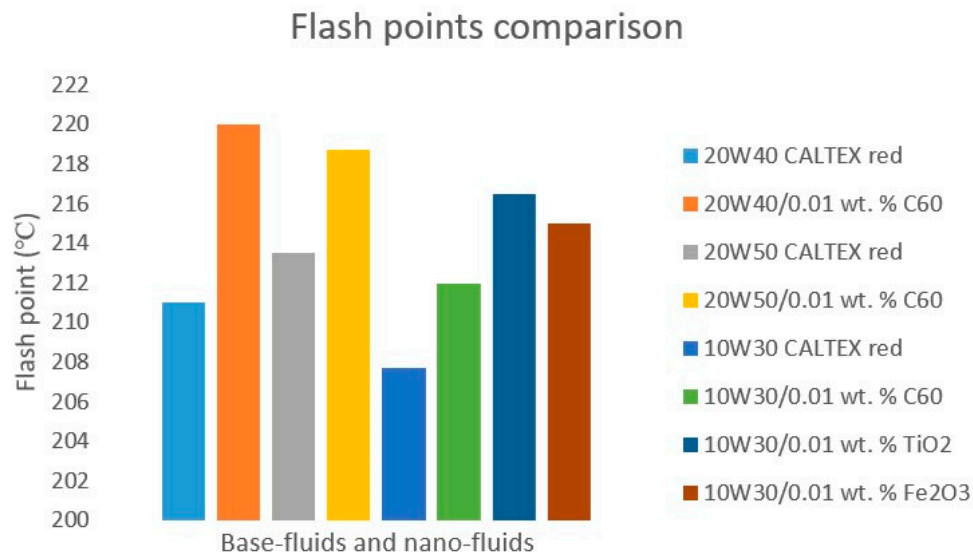
Figure 11. Effect of volumetric heat capacity on 10W30/Fe$_2$O$_3$ 0.01 wt.% added nano-fluid.

All graphs were linear, while volumetric heat capacity vs. temperature graphs kept a positive gradient**.**

3.2.4. Flash point

Table 5 and Figure 12 present a comparison of the flash point values of three different graded engine oils with their relevant fullerene-C$_{60}$, TiO$_2$, and Fe$_2$O$_3$-added nanofluids. The results proved a considerable impact on the flash point of engine oil with 0.01 wt.% of fullerene-C$_{60}$, TiO$_2$, and Fe$_2$O$_3$ nanomaterials. The effect on the flash point regarding three engine oil grades was approximately equal. However, when comparing the effect on the flash points from nanomaterials, it was observed that a decrement with TiO$_2$, Fe$_2$O$_3$, and fullerene-C$_{60}$, respectively.

Figure 12. The comparison of flash point values of three different engine oil with their nano-fluids.

3.3. Thermal property ratios

This section presents the ratio of thermal conductivity, thermal diffusivity, volumetric heat capacity, and flash point of nanofluid to the base fluid.

3.3.1. Thermal conductivity, Thermal diffusivity, and Volumetric heat capacity ratios

The ratios of thermal conductivity, thermal diffusivity, and volumetric heat capacity can be calculated using Eq. (4), Eq. (5), and Eq. (6), respectively.

$$Thermal\ conductivity\ ratio(\%) = \left(\left(\lambda_{nf} - \lambda_{bf}\right)/\lambda_{bf}\right) \times 100\% \tag{4}$$

$$Thermal\ diffusivity\ ratio(\%) = \left(\left(\alpha_{nf} - \alpha_{bf}\right)/\alpha_{bf}\right) \times 100\% \tag{5}$$

$$Volumetric\ heat\ capacity\ ratio(\%) = \left(\left(Cv_{nf} - Cv_{bf}\right)/Cv_{bf}\right) \times 100\% \tag{6}$$

3.3.2. Flash point ratio

$$Flash\ point\ ratio(\%) = \left(\left(\beta_{nf} - \beta_{bf}\right)/\beta_{bf}\right) \times 100\% \tag{7}$$

The flashpoint ratio can be calculated by referring to Eq. (7) and the nanofluid based on TiO$_2$ with 0.01 wt.%.   Exhibits the highest flash point ratio.

Table 5 represents the maximum enhancements in the thermal properties of nanofluids.

Table 5. Maximum thermal property ratios of 10W30/nanofluids Fullerene-C$_{60}$, TiO$_2$, and Fe$_2$O$_3$ at 0.01 wt.%.

| Thermal property	Fullerene-C$_{60}$ based nanofluid	TiO$_2$ based nanofluid	Fe$_2$O$_3$ based nanofluid
Thermal conductivity ratio (%)	-	4.5	3.9
Thermal diffusivity ratio (%)	-	0.6	0.5
Volumetric heat capacity ratio (%)	-	3.7	3.4
Flashpoint ratio (%)	2.1	4.2	3.5

3.4. Correlations of thermal properties

According to the literature, the thermal and physical properties of nanofluids depend on different factors such as characteristics of nanoparticles (size, shape, material), nanoparticle concentration, temperature, surfactant, base fluid, nanofluid preparation method, and ultrasonication and stirring duration [37–51]. Figures 13–16 compare the thermal properties of 10W30-based. These charts represent the thermal properties of the nano lubricant using different nanomaterials at a temperature range of 30-120 ℃.
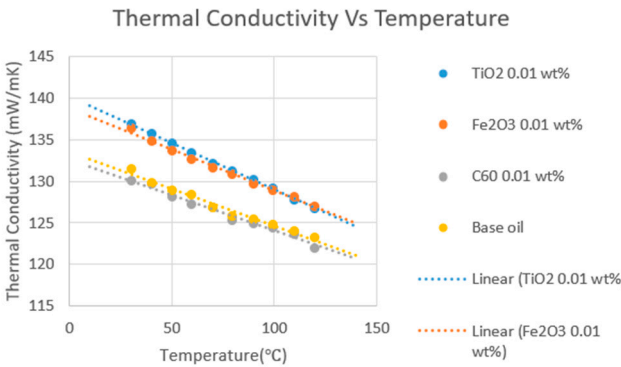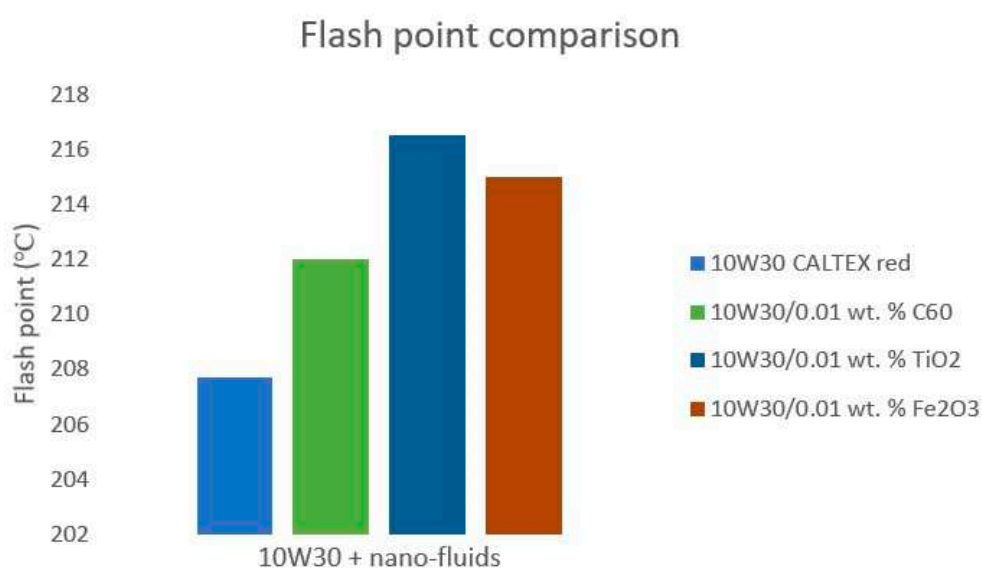

Figure 13. Effect of thermal conductivity on 10W30/nanoparticles with mass fraction 0.01 wt.%.
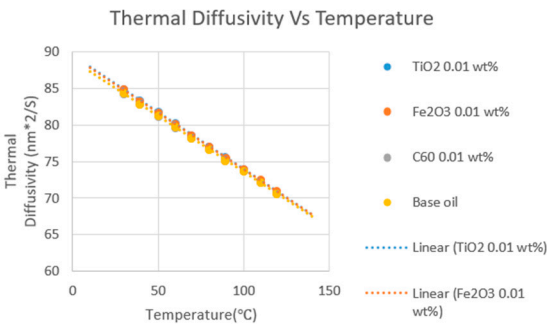
Figure 14. Effect of thermal diffusivity on 10W30/nanoparticles with mass fraction 0.01 wt.%.
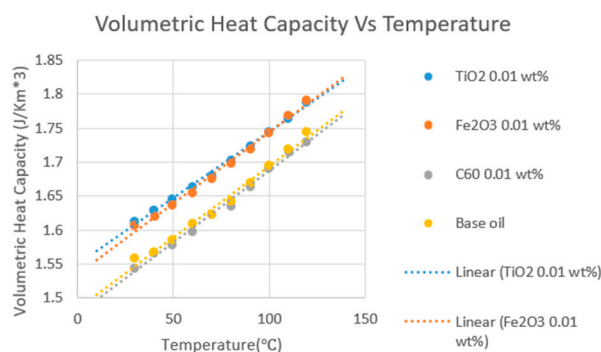
Figure 15. Effect of volumetric heat capacity on 10W30/nanoparticles with mass fraction 0.01 wt.%.

Figure 16. Flash point comparison of 10W30 based nano-fluids (0.01 wt.%).

4. Conclusions

The numerous applications, economic and energy efficiency matter to improve the thermal properties of engine oil by the addition of nanoparticles. This research work described the preparation procedure of nanofluids, fullerene-C_{60}/10W30, fullerene-C_{60}/20W40, fullerene-C_{60}/20W50, TiO_2/10W30, and Fe_2O_3/10W30. The thermal properties, including thermal conductivity, thermal diffusivity, volumetric heat capacity, and flash point, were investigated in each nanofluid sample as a function of temperature range of 30-120 °C and mass fraction of 0.01 wt.%.

Even though the low mass fraction was used in this study, the stability of the nanofluids' was acceptable, and surfactants were not required. The two-step preparation method with magnetic stirring, ultrasonic waves, and heating process helped to prevent sedimentation and agglomeration. There was no requirement for a surfactant to stabilize the nanofluid.

The following observations were obtained through the experimental results.

- The thermal properties of engine oil-based nanofluids of metal oxide nanoparticles (TiO_2 and Fe_2O_3) displayed significant increments compared to their respective base fluids.
- The TiO_2/10W30 nanofluid showed the highest percentage increment of thermal properties in this experiment, where 4.5% thermal conductivity ratio at a temperature of 40 °C, 0.6% thermal diffusivity ratio at a temperature of 50 °C, 3.7% of volumetric heat capacity ratio at a temperature 50 °C, and 4.2% of flash point ratio.
- The Fe_2O_3/10W30 nanofluid was proved to have a 3.9% thermal conductivity ratio at a temperature 80 °C, 0.5% of thermal diffusivity ratio at temperature range 30-80 °C, 3.4% of

volumetric heat capacity ratio at temperature 80 ℃, and 3.5% of flash point ratio where it's observed that Fe_2O_3/10W30 nanofluid has better thermal properties in higher temperatures compared to TiO_2/10W30 nanofluid.

- The fullerene-C_{60}-based nanofluids exhibited a notable increase of 2.1% in flash points while not showing significant enhancements in the other thermal properties.

It can be concluded that the thermal properties of engine oils can be enhanced using both metal oxide nanoparticles (TiO_2 and Fe_2O_3) and fullerene-C_{60} nanoparticles. The thermal property enhancement ability of metal oxide nanoparticles is comparatively higher than fullerene-C_{60} nanoparticles in nanofluids.

Conflicts of Interest: The authors declare no conflict of interest.

References

1. Tahmasebi Sulgani, M.; Karimipour, A. Improve the Thermal Conductivity of 10w40-Engine Oil at Various Temperature by Addition of Al2O3/Fe2O3 Nanoparticles. *J. Mol. Liq.* **2019**, *283*, 660–666. https://doi.org/10.1016/j.molliq.2019.03.140.
2. Nojoomizadeh, M.; Karimipour, A. The Effects of Porosity and Permeability on Fluid Flow and Heat Transfer of Multi Walled Carbon Nano-Tubes Suspended in Oil (MWCNT/Oil Nano-Fluid) in a Microchannel Filled with a Porous Medium. *Phys. E Low-Dimens. Syst. Nanostructures* **2016**, *84*, 423–433. https://doi.org/10.1016/j.physe.2016.07.020.
3. (PDF) 123137893-Lubricant-Additives-Chemistry-and-Applications | Abdou Benkirane - Academia.Edu Available online: https://www.academia.edu/3892345/123137893_lubricant_additives_chemistry_and_applications (accessed on 11 October 2023).
4. Asadi, A.; Asadi, M.; Rezaniakolaei, A.; Rosendahl, L.A.; Wongwises, S. An Experimental and Theoretical Investigation on Heat Transfer Capability of Mg (OH)2/MWCNT-Engine Oil Hybrid Nano-Lubricant Adopted as a Coolant and Lubricant Fluid. *Appl. Therm. Eng.* **2018**, *129*, 577–586. https://doi.org/10.1016/j.applthermaleng.2017.10.074.
5. Ranjbarzadeh, R.; Karimipour, A.; Afrand, M.; Isfahani, A.H.M.; Shirneshan, A. Empirical Analysis of Heat Transfer and Friction Factor of Water/Graphene Oxide Nanofluid Flow in Turbulent Regime through an Isothermal Pipe. *Appl. Therm. Eng.* **2017**, *126*, 538–547. https://doi.org/10.1016/j.applthermaleng.2017.07.189.
6. Das, S.K.; Choi, S.U.S.; Patel, H.E. Heat Transfer in Nanofluids—A Review. *Heat Transf. Eng.* **2006**, *27*, 3–19. https://doi.org/10.1080/01457630600904593.
7. Ghasemi, S.; Karimipour, A. Experimental Investigation of the Effects of Temperature and Mass Fraction on the Dynamic Viscosity of CuO-Paraffin Nanofluid. *Appl. Therm. Eng.* **2018**, *128*, 189–197. https://doi.org/10.1016/j.applthermaleng.2017.09.021.
8. Koca, H.D.; Doganay, S.; Turgut, A.; Tavman, I.H.; Saidur, R.; Mahbubul, I.M. Effect of Particle Size on the Viscosity of Nanofluids: A Review. *Renew. Sustain. Energy Rev.* **2018**, *82*, 1664–1674. https://doi.org/10.1016/j.rser.2017.07.016.
9. Hamzah, M.H.; Sidik, N.A.C.; Ken, T.L.; Mamat, R.; Najafi, G. Factors Affecting the Performance of Hybrid Nanofluids: A Comprehensive Review. *Int. J. Heat Mass Transf.* **2017**, *115*, 630–646. https://doi.org/10.1016/j.ijheatmasstransfer.2017.07.021.
10. Ranjbarzadeh, R.; Meghdadi Isfahani, A.H.; Afrand, M.; Karimipour, A.; Hojaji, M. An Experimental Study on Heat Transfer and Pressure Drop of Water/Graphene Oxide Nanofluid in a Copper Tube under Air Cross-Flow: Applicable as a Heat Exchanger. *Appl. Therm. Eng.* **2017**, *125*, 69–79. https://doi.org/10.1016/j.applthermaleng.2017.06.110.

11. Pavía, M.; Alajami, K.; Estellé, P.; Desforges, A.; Vigolo, B. A Critical Review on Thermal Conductivity Enhancement of Graphene-Based Nanofluids. *Adv. Colloid Interface Sci.* **2021**, *294*, 102452. https://doi.org/10.1016/j.cis.2021.102452.

12. Ettefaghi, E.; Rashidi, A.; Ahmadi, H.; Mohtasebi, S.S.; Pourkhalil, M. Thermal and Rheological Properties of Oil-Based Nanofluids from Different Carbon Nanostructures. *Int. Commun. Heat Mass Transf.* **2013**, *48*, 178–182. https://doi.org/10.1016/j.icheatmasstransfer.2013.08.004.

13. Rostamian, S.H.; Saedodin, S.; Asgari, S.A.; Salarian, A.H. Effect of C60-SiO2 Hybrid Nanoparticles on Thermophysical and Tribological Properties of a Multigrade Engine Oil: An Experimental Study. *J. Therm. Anal. Calorim.* **2022**, *147*, 155–167. https://doi.org/10.1007/s10973-020-10323-8.

14. Sukkar, K.A.; Karamalluh, A.A.; Jaber, T.N. Rheological and Thermal Properties of Lubricating Oil Enhanced by the Effect of CuO and TiO2 Nano-Additives. *Al-Khwarizmi Eng. J.* **2019**, *15*, 24–33. https://doi.org/10.22153/kej.2019.12.002.

15. Birleanu, C.; Pustan, M.; Cioaza, M.; Molea, A.; Popa, F.; Contiu, G. Effect of TiO2 Nanoparticles on the Tribological Properties of Lubricating Oil: An Experimental Investigation. *Sci. Rep.* **2022**, *12*, 5201. https://doi.org/10.1038/s41598-022-09245-2.

16. Sarbolookzadeh Harandi, S.; Karimipour, A.; Afrand, M.; Akbari, M.; D'Orazio, A. An Experimental Study on Thermal Conductivity of F-MWCNTs–Fe 3 O 4 /EG Hybrid Nanofluid: Effects of Temperature and Concentration. *Int. Commun. Heat Mass Transf.* **2016**, *76*, 171–177. https://doi.org/10.1016/j.icheatmasstransfer.2016.05.029.

17. D15 Committee *Test Method for Thermal Conductivity, Thermal Diffusivity and Volumetric Heat Capacity of Engine Coolants and Related Fluids by Transient Hot Wire Liquid Thermal Conductivity Method*; ASTM International;

18. D93 Standard Test Methods for Flash Point by Pensky-Martens Closed Cup Tester Available online: https://www.astm.org/d0093-20.html (accessed on 11 October 2023).

19. Wei, B.; Zou, C.; Li, X. Experimental Investigation on Stability and Thermal Conductivity of Diathermic Oil Based TiO2 Nanofluids. *Int. J. Heat Mass Transf.* **2017**, *104*, 537–543. https://doi.org/10.1016/j.ijheatmasstransfer.2016.08.078.

20. Abid, M.A.; Khan, I.; Ullah, Z.; Ullah, K.; Haider, A.; Ali, S.M. Dielectric and Thermal Performance Up-Gradation of Transformer Oil Using Valuable Nano-Particles. *IEEE Access* **2019**, *7*, 153509–153518. https://doi.org/10.1109/ACCESS.2019.2948959.

21. Aberoumand, S.; Jafarimoghaddam, A. Experimental Study on Synthesis, Stability, Thermal Conductivity and Viscosity of Cu–Engine Oil Nanofluid. *J. Taiwan Inst. Chem. Eng.* **2017**, *71*, 315–322. https://doi.org/10.1016/j.jtice.2016.12.035.

22. Asadi, M.; Asadi, A.; Aberoumand, S. An Experimental and Theoretical Investigation on the Effects of Adding Hybrid Nanoparticles on Heat Transfer Efficiency and Pumping Power of an Oil-Based Nanofluid as a Coolant Fluid. *Int. J. Refrig.* **2018**, *89*, 83–92. https://doi.org/10.1016/j.ijrefrig.2018.03.014.

23. Aberoumand, S.; Jafarimoghaddam, A. Tungsten (III) Oxide (WO 3) – Silver/Transformer Oil Hybrid Nanofluid: Preparation, Stability, Thermal Conductivity and Dielectric Strength. *Alex. Eng. J.* **2018**, *57*, 169–174. https://doi.org/10.1016/j.aej.2016.11.003.

24. Ettefaghi, E.; Ahmadi, H.; Rashidi, A.; Nouralishahi, A.; Mohtasebi, S.S. Preparation and Thermal Properties of Oil-Based Nanofluid from Multi-Walled Carbon Nanotubes and Engine Oil as Nano-Lubricant. *Int. Commun. Heat Mass Transf.* **2013**, *46*, 142–147. https://doi.org/10.1016/j.icheatmasstransfer.2013.05.003.

25. Sathishkumar, S.D.; Rajmohan, T. Preparation and Analysis of the Thermal Properties of Engine Oil Reinforced with Multi-Walled Carbon Nanotubes. *IOP Conf. Ser. Mater. Sci. Eng.* **2018**, *390*, 012068. https://doi.org/10.1088/1757-899X/390/1/012068.

26. Aberoumand, S.; Jafarimoghaddam, A.; Moravej, M.; Aberoumand, H.; Javaherdeh, K. Experimental Study on the Rheological Behavior of Silver-Heat Transfer Oil Nanofluid and Suggesting Two Empirical Based Correlations for Thermal Conductivity and Viscosity of Oil Based Nanofluids. *Appl. Therm. Eng.* **2016**, *101*, 362–372. https://doi.org/10.1016/j.applthermaleng.2016.01.148.

27. Farbod, M.; Kouhpeymani Asl, R.; Noghreh Abadi, A.R. Morphology Dependence of Thermal and Rheological Properties of Oil-Based Nanofluids of CuO Nanostructures. *Colloids Surf. Physicochem. Eng. Asp.* **2015**, *474*, 71–75. https://doi.org/10.1016/j.colsurfa.2015.02.049.

28. Ettefaghi, E.; Ahmadi, H.; Rashidi, A.; Mohtasebi, S.S.; Alaei, M. Experimental Evaluation of Engine Oil Properties Containing Copper Oxide Nanoparticles as a Nanoadditive. *Int. J. Ind. Chem.* **2013**, *4*, 28. https://doi.org/10.1186/2228-5547-4-28.

29. Yu, W.; Xie, H.; Wang, X.; Wang, X. Significant Thermal Conductivity Enhancement for Nanofluids Containing Graphene Nanosheets. *Phys. Lett. A* **2011**, *375*, 1323–1328. https://doi.org/10.1016/j.physleta.2011.01.040.

30. Ranjbarzadeh, R.; Chaabane, R. Experimental Study of Thermal Properties and Dynamic Viscosity of Graphene Oxide/Oil Nano-Lubricant. *Energies* **2021**, *14*, 2886. https://doi.org/10.3390/en14102886.

31. Agarwal, D.K.; Vaidyanathan, A.; Sunil Kumar, S. Experimental Investigation on Thermal Performance of Kerosene–Graphene Nanofluid. *Exp. Therm. Fluid Sci.* **2016**, *71*, 126–137. https://doi.org/10.1016/j.expthermflusci.2015.10.028.

32. Alqahtani, B.; Hoziefa, W.; Abdel Moneam, H.M.; Hamoud, M.; Salunkhe, S.; Elshalakany, A.B.; Abdel-Mottaleb, M.; Davim, J.P. Tribological Performance and Rheological Properties of Engine Oil with Graphene Nano-Additives. *Lubricants* **2022**, *10*, 137. https://doi.org/10.3390/lubricants10070137.

33. Li, Z.; Asadi, S.; Karimipour, A.; Abdollahi, A.; Tlili, I. Experimental Study of Temperature and Mass Fraction Effects on Thermal Conductivity and Dynamic Viscosity of SiO2-Oleic Acid/Liquid Paraffin Nanofluid. *Int. Commun. Heat Mass Transf.* **2020**, *110*, 104436. https://doi.org/10.1016/j.icheatmasstransfer.2019.104436.

34. Desai, N.; Nagaraj, A.M.; Sabnis, N. Analysis of Thermo-Physical Properties of SAE20W40 Engine Oil by the Addition of SiO2 Nanoparticles. *Mater. Today Proc.* **2021**, *47*, 5646–5651. https://doi.org/10.1016/j.matpr.2021.03.688.

35. Khalil, W.; Mohamed, A.; Bayoumi, M.; Osman, T.A. Thermal and Rheological Properties of Industrial Mineral Gear Oil and Paraffinic Oil/CNTs Nanolubricants. *Iran. J. Sci. Technol. Trans. Mech. Eng.* **2018**, *42*, 355–361. https://doi.org/10.1007/s40997-017-0103-3.

36. Yang, L.; Mao, M.; Huang, J.; Ji, W. Enhancing the Thermal Conductivity of SAE 50 Engine Oil by Adding Zinc Oxide Nano-Powder: An Experimental Study. *Powder Technol.* **2019**, *356*, 335–341. https://doi.org/10.1016/j.powtec.2019.08.031.

37. Yu, W.; Xie, H.; Bao, D. Enhanced Thermal Conductivities of Nanofluids Containing Graphene Oxide Nanosheets. *Nanotechnology* **2010**, *21*, 055705. https://doi.org/10.1088/0957-4484/21/5/055705.

38. Simpson, S.; Schelfhout, A.; Golden, C.; Vafaei, S. Nanofluid Thermal Conductivity and Effective Parameters. *Appl. Sci.* **2018**, *9*, 87. https://doi.org/10.3390/app9010087.

39. Jia, L.; Chen, Y.; Lei, S.; Mo, S.; Luo, X.; Shao, X. External Electromagnetic Field-Aided Freezing of CMC-Modified Graphene/Water Nanofluid. *Appl. Energy* **2016**, *162*, 1670–1677. https://doi.org/10.1016/j.apenergy.2015.08.067.

40. Taherialekouhi, R.; Rasouli, S.; Khosravi, A. An Experimental Study on Stability and Thermal Conductivity of Water-Graphene Oxide/Aluminum Oxide Nanoparticles as a Cooling Hybrid Nanofluid. *Int. J. Heat Mass Transf.* **2019**, *145*, 118751. https://doi.org/10.1016/j.ijheatmasstransfer.2019.118751.

41. Karimipour, A.; Taghipour, A.; Malvandi, A. Developing the Laminar MHD Forced Convection Flow of Water/FMWNT Carbon Nanotubes in a Microchannel Imposed the Uniform Heat Flux. *J. Magn. Magn. Mater.* **2016**, *419*, 420–428. https://doi.org/10.1016/j.jmmm.2016.06.063.

42. Goodarzi, M.; Safaei, M.R.; Oztop, H.F.; Karimipour, A.; Sadeghinezhad, E.; Dahari, M.; Kazi, S.N.; Jomhari, N. Numerical Study of Entropy Generation Due to Coupled Laminar and Turbulent Mixed Convection and Thermal Radiation in an Enclosure Filled with a Semitransparent Medium. *Sci. World J.* **2014**, *2014*, e761745. https://doi.org/10.1155/2014/761745.

43. Hemmat Esfe, M.; Abbasian Arani, A.A.; Niroumand, A.H.; Yan, W.-M.; Karimipour, A. Mixed Convection Heat Transfer from Surface-Mounted Block Heat Sources in a Horizontal Channel with Nanofluids. *Int. J. Heat Mass Transf.* **2015**, *89*, 783–791. https://doi.org/10.1016/j.ijheatmasstransfer.2015.05.100.

44. Akbari, M.; Afrand, M.; Arshi, A.; Karimipour, A. An Experimental Study on Rheological Behavior of Ethylene Glycol Based Nanofluid: Proposing a New Correlation as a Function of Silica Concentration and Temperature. *J. Mol. Liq.* **2017**, *233*, 352–357. https://doi.org/10.1016/j.molliq.2017.03.020.

45. Khodadadi, H.; Toghraie, D.; Karimipour, A. Effects of Nanoparticles to Present a Statistical Model for the Viscosity of MgO-Water Nanofluid. *Powder Technol.* **2019**, *342*, 166–180. https://doi.org/10.1016/j.powtec.2018.09.076.

46. Shahsavar, A.; Khanmohammadi, S.; Karimipour, A.; Goodarzi, M. A Novel Comprehensive Experimental Study Concerned Synthesizes and Prepare Liquid Paraffin-Fe3O4 Mixture to Develop Models for Both Thermal Conductivity & Viscosity: A New Approach of GMDH Type of Neural Network. *Int. J. Heat Mass Transf.* **2019**, *131*, 432–441. https://doi.org/10.1016/j.ijheatmasstransfer.2018.11.069.

47. Karimipour, A.; Hemmat Esfe, M.; Safaei, M.R.; Toghraie Semiromi, D.; Jafari, S.; Kazi, S.N. Mixed Convection of Copper–Water Nanofluid in a Shallow Inclined Lid Driven Cavity Using the Lattice Boltzmann Method. *Phys. Stat. Mech. Its Appl.* **2014**, *402*, 150–168. https://doi.org/10.1016/j.physa.2014.01.057.

48. Karimipour, A.; Hossein Nezhad, A.; D'Orazio, A.; Hemmat Esfe, M.; Safaei, M.R.; Shirani, E. Simulation of Copper–Water Nanofluid in a Microchannel in Slip Flow Regime Using the Lattice Boltzmann Method. *Eur. J. Mech. - BFluids* **2015**, *49*, 89–99. https://doi.org/10.1016/j.euromechflu.2014.08.004.

49. Nafchi, P.M.; Karimipour, A.; Afrand, M. The Evaluation on a New Non-Newtonian Hybrid Mixture Composed of TiO 2 /ZnO/EG to Present a Statistical Approach of Power Law for Its Rheological and Thermal Properties. *Phys. Stat. Mech. Its Appl.* **2019**, *516*, 1–18. https://doi.org/10.1016/j.physa.2018.10.015.

50. Alrashed, A.A.A.A.; Karimipour, A.; Bagherzadeh, S.A.; Safaei, M.R.; Afrand, M. Electro- and Thermophysical Properties of Water-Based Nanofluids Containing Copper Ferrite Nanoparticles Coated with Silica: Experimental Data, Modeling through Enhanced ANN and Curve Fitting. *Int. J. Heat Mass Transf.* **2018**, *127*, 925–935. https://doi.org/10.1016/j.ijheatmasstransfer.2018.07.123.

51. Karimipour, A.; Bagherzadeh, S.A.; Goodarzi, M.; Alnaqi, A.A.; Bahiraei, M.; Safaei, M.R.; Shadloo, M.S. Synthesized CuFe2O4/SiO2 Nanocomposites Added to Water/EG: Evaluation of the Thermophysical Properties beside Sensitivity Analysis & EANN. *Int. J. Heat Mass Transf.* **2018**, *127*, 1169–1179. https://doi.org/10.1016/j.ijheatmasstransfer.2018.08.112.